



Published in final edited form as:

*Transl Res.* 2019 September ; 211: 46–63. doi:10.1016/j.trsl.2019.04.002.

## Recent Advances in 3D Printing: Vascular Network for Tissue and Organ Regeneration

Sung Yun Hann<sup>1</sup>, Haitao Cui<sup>1</sup>, Timothy Esworthy<sup>1</sup>, Shida Miao<sup>1</sup>, Xuan Zhou<sup>1</sup>, Se-jun Lee<sup>1</sup>, John P. Fisher<sup>2,3</sup>, Lijie Grace Zhang<sup>1,4,5,6</sup>

<sup>1</sup>Department of Mechanical and Aerospace Engineering, The George Washington University, Washington, DC 20052, USA

<sup>2</sup>Fischell Department of Bioengineering, University of Maryland, College Park, MD 20742, USA

<sup>3</sup>Center for Engineering Complex Tissues, University of Maryland, College Park, MD 20742, USA

<sup>4</sup>Department of Electrical and Computer Engineering, The George Washington University, Washington, DC 20052, USA

<sup>5</sup>Department of Biomedical Engineering, The George Washington University, Washington, DC 20052, USA

<sup>6</sup>Department of Medicine, The George Washington University Medical Center, Washington, DC 20052, USA

### Abstract

Over the past years, the fabrication of adequate vascular networks has remained the main challenge in engineering tissues due to technical difficulties, while the ultimate objective of tissue engineering is to create fully functional and sustainable organs and tissues to transplant in the human body. There have been a number of studies performed to overcome this limitation, and as a result, 3D printing has become an emerging technique to serve in a variety of applications in constructing vascular networks within tissues and organs. 3D printing incorporated technical approaches allow researchers to fabricate complex and systematic architecture of vascular networks and offer various selections for fabrication materials and printing techniques. In this review, we will discuss materials and strategies for 3D printed vascular networks as well as specific applications for certain vascularized tissue and organ regeneration. We will also address the current limitations of vascular tissue engineering and make suggestions for future directions research may take.

---

**Corresponding Author:** Lijie Grace Zhang, Ph.D., Associate Professor, Department of Mechanical and Aerospace Engineering, The George Washington University, Science and Engineering Hall 3590, 800 22nd Street NW, Washington DC 20052, lgzhang@email.gwu.edu.

**Publisher's Disclaimer:** This is a PDF file of an unedited manuscript that has been accepted for publication. As a service to our customers we are providing this early version of the manuscript. The manuscript will undergo copyediting, typesetting, and review of the resulting proof before it is published in its final citable form. Please note that during the production process errors may be discovered which could affect the content, and all legal disclaimers that apply to the journal pertain.

## Keywords

3D printing; vascular network; tissue and organ regeneration; biomaterials; biofabrication

---

## 1. Introduction

The primary aim of tissue engineering is to develop fully functional and sustainable tissues and organs *in vitro* and *in vivo* for repairing or replacing damaged tissues in the body (1–4). Approaches involved in tissue engineering have varied among their specific applications such as regeneration of bone, skin, heart, and others (5). Although there have been many studies performed in that regard, only a few of them have presented successful results from the *in vitro* level to clinical transplantation (6, 7). The lack of acquired data in tissue engineering mainly originates from insufficient technical advancement in the creation of blood vessels, which are referred to as vascularized networks (8). Vascularization is essential for the supplementation of oxygen and nutrients, as well as the removal of waste, which is necessary for tissues and organs to maintain their functions (5, 9). In general, vascular networks can be created via vasculogenesis and angiogenesis (9). Vasculogenesis involves the generation of new blood vessels from endothelial cells (ECs), whereas angiogenesis is assisted by germination from existing vessels (9).

Many techniques have been adopted to fabricate vascular networks with complex, unique structures and functionality for mimicking blood vessels in the human body so far; however, 3D printing techniques have attracted researchers particularly during the past years due to outstanding advantages including controllability, reproducibility, and repeatability (5). Since 3D printing was first developed in the 1980s, there have been enormous advancements in tissue and organ regeneration (10, 11). As a result, it has become common to generate vascular networks in organs or tissues by utilizing several different 3D printing techniques with a varied selection of materials due to its quickness compared to microcirculation *in vivo* (5). However, 3D printed vascularization still remains a challenge since it has been unable to fully mimic the complex structure and function of natural vasculature.

In this review, we focus on 3D printing techniques, materials, and other elements that are taken into account for the successful formation of vascular networks with relevant applications as means to discuss the current limitations of vascular tissue engineering and to propose future research directions.

## 2. 3D Printing Methods for Vascular Fabrication

Although the fabrication of perfectly functional vascular networks remains a challenge for most tissue engineers (12), there are considerable types of 3D printing methods that are expected to overcome current limitations. Commonly, many researchers have categorized 3D printing into two types by cell seeding method: Direct-Cell-Seeding and Post-Cell-Seeding by incorporating laser-assisted, droplet-based, and extrusion-based manufacturing processes (5, 13). Regarding the methodologies to create vascular constructs, there are two major approaches that can be taken into consideration. First, vascularization promoting cells can be co-cultured within the scaffolds to generate vascular networks. Second, perfusable blood

vessels can be created via direct fabrication. Specifically, in the fabrication of 3D vascular networks, it is conventional to utilize extrusion-based and stereolithography apparatus (SLA) printing techniques.

Extrusion-based techniques including fused deposition modeling (FDM) and bioplotting are the most universally used 3D printing platforms for direct writing. The FDM technique employs ample heating for the transition of materials from solid to the semi-molten state before solidification at the time of printing (10). It is compatible with a wide selection of plastic biomaterials and offers great versatility in the study of 3D printing in general. However, FDM also possesses some drawbacks such as a notably limited printing resolution and restriction of hydrogel use. For example, the minimum feature size of 100  $\mu\text{m}$  and compulsory “molten-solid” state transition for the extrusion step are considerable downsides compared to other 3D printing strategies (14). Comparatively, bioplotting is a fluid-dispensing system, capable of employing a wide selection of cell-laden bioinks such as cell aggregates, hydrogels, micro-carriers, and decellularized matrices (5).

SLA involves a surface photopolymerization of a liquid or gel state polymer induced by an ultraviolet (UV) laser. SLA primarily utilizes laser energy to generate subsequently thick and solidified layers in the bioink reservoir. Although scaffolds created by SLA are not mechanically robust, this strategy offers precise control of resolution accompanied by a microscale laser tip. Unlike FDM, SLA offers a limited selection for bioinks that must be photopolymerizable. To date, modification of polymers has been investigated to overcome this restriction, but the number of bioinks are still limited compared to FDM (10). Also, an excessive exposure to the UV light can result in geometrical distortion or shrinkage (10).

Here, we focus on the methods to create perfusable 3D vascular networks by classifying them into two different regimes, direct and indirect printing systems, where the most important aspect in 3D printing vascular networks is biomimicry and implementing their complex and hierarchical design (Figure 1 and Table 1).

## 2.1 Direct Printing

The first approach is direct patterning to implement internal tubular shapes within a scaffold. This approach requires fewer fabrication steps as it performs the creation of blood vessels and tissue in a continuous, layer-by-layer process. All printing systems mentioned above can be utilized for direct printing. Therefore, to date, there have been a variety of studies performed to demonstrate vascularized tissue and organ regenerations using this method. For example, the study done by Suri *et al.* utilized a method in which partially UV cured photopolymerizable glycidyl methacrylate hyaluronic acid (GMHA) was used to fabricate a microchannel incorporated 3D scaffold. Selective reflection of UV light using the pre-patterned substrate under the SLA system led to partial photopolymerization of the ink. A sequential deposition-wash off-deposition process between each layer was incorporated (15). Also, different microscale structures with various inner shapes were printable in polyethylene glycol diacrylate (PEGDA) and lithium phenyl-2, 4, 6-trimethylbenzoylphosphinate (LAP) using SLA (16). In addition, Laschke *et al.* utilized a 3D bioplotting technique to fabricate polylactic-glycolic acid (PLGA) based scaffolds in order to create vascular networks capable of angiogenesis in the presence of growth factor

(17). The notorious issue with direct horizontal 3D printing is an erratic fluid stream within printed internal microchannels due to blockage or pleated shape caused by gravity (18). Another interesting direct 3D printing platform was recently introduced by Hinton *et al.* They modified a thermoplastic extrusion-based 3D printer by adding a custom-built syringe pump extrusion system to it (19). The system incorporated a thermo-reversible support bath with gelatin microparticles for specialized use in 3D printing of hydrogel bioinks in a layer-by-layer fashion. Upon the completion of printing, sufficient heating removed the gelatin support, leaving only the printed structure. The authors showed that this modified extrusion 3D printer was capable of fabricating complex geometrical structures, such as coronary artery vascular trees and embryonic chick heart (19). Thus, this platform can be considered useful for 3D printing of complex biological structures with hydrogels.

## 2.2 Indirect Printing

The utilization of a sacrificial template that leads to indirect printing overcomes the main drawback of direct patterning on the substrate. Golden *et al.* fabricated a minimum of 6  $\mu\text{m}$  wide internal channel using the liquefaction temperature difference between the Polydimethylsiloxane (PDMS) substrate and the gelatin mesh that they used. In their study, heating at room temperature for 1 hour was substantial to allow the gelatin to melt. As a result, scaffolds with hollow microchannels consisting of open ends were fabricated (20). Similarly, multiple studies utilized gelatin as an impermanent template to generate vascular channels within collagen-based tissue structures (21, 22). In one of the earlier studies, Wu *et al.* printed a 3D microvascular network using thermal and chemical characteristics of a fugitive ink consist of Pluronic® F127 (23). Although the use of a sacrificial template suggests an advantage over the direct printing methods in the aforementioned geometrical and microfluidic aspects, as it is still left with constraints in fabrication and feasibility during and after printing. First, this approach is surrounding hydrogel or polymer construct dependent, thereby precise control on the outer material are restricted (5). Second, an efficient method to interconnect the vessels with a complicated design to mimic the natural vascular network needs to be resolved. The previously performed studies are mostly implementable to vascularized networks which lie horizontally between the layers or simply stack vertically, which is a limited approach to model the complex design of native vascularized networks.

## 3. Material and Cell Selections

The next aspect of 3D printing is the selection of versatile bioinks and cells. There are properties required that biomaterials must fulfill in order to achieve a desired 3D printed construct with its biological functionalization. Above all, biomaterials should exhibit suitability to implement innate features of native blood vessels, which are composed of collagen and elastic fibers, elastic lamellae, and proteoglycans (24). Besides bearing resemblances to the material properties of native blood vessels, a bioink must also have characteristics which can be explicitly summarized in terms of printability, biocompatibility, biodegradability, and suitable mechanical properties. Among various groups of chemicals, polymers occupy the majority of conventional bioinks due to the possession of the listed properties above. Polymers for bioinks are divided into two major categories by their

origins, natural and synthetic (Table 2). The natural polymers are naturally obtained or extracted from humans, animals, bacteria, or plants, whereas synthetic polymers are man-made and intentionally synthesized to supplement the drawbacks of natural polymers, which will be discussed in the following sub-sections. To formulate a suitable bioink, there are a number of biological and mechanical characteristics of the materials which must be taken into consideration. Regardless of the classification, the bioink should exhibit degradability and biocompatibility for cell proliferation and growth as well as printability (10). Especially in the case of vascular fabrication, shape fidelity, stability (e.g., swelling) and flexibility are also some considerable requirements for material selection as they are directly relevant to the sustainability of tubular and pore structures (10). According to the “biofabrication window” described by Malda *et al.* and Sun *et al.*, the printability of bioinks is proportional to polymer concentration, which affects crosslinkability and shape fidelity for 3D printing of vascular networks (25, 26). However, a densely crosslinked environment interferes with cell viability, which means the degree of biocompatibility of the printed construct is constrained by its mechanical properties (25). Therefore, moderate crosslinking of the biopolymer is necessary to obtain suitable biological and mechanical properties.

In addition to the listed properties of bioinks, microenvironmental conditions must be considered for the initiation of vasculogenesis and angiogenesis. For example, one of the cell types to be discussed in the following section, endothelial progenitor cells (EPCs), have been shown to be influenced by laminar shear stress, which in turn promotes vasculogenesis. (27). According to the study by Yamamoto *et al.*, laminar shear stress was found to stimulate EPC proliferation and morphological changes. Thus, vasculogenesis was promoted in dynamic culture conditions, while greater angiogenesis was observed in static conditions (27). Another microenvironmental condition for ECs to form vascular networks is the inclusion of bioactive growth factors, such as the use of vascular endothelial growth factor (VEGF) (28). Although concentrations of VEGF outside of the ideal range may result in abnormal constructs, proper use of VEGF is crucial to accelerate the formation of vascular networks (28).

### 3.1 Natural Polymers

Natural polymers are widely used as the fundamental elements to obtain biomimetic characteristics of the extracellular matrix (ECM), which is considered the biggest advantage. However, there are noteworthy drawbacks to natural polymers as well, such as their lack of mechanical strength and controllability over their chemical structure (5). Selection of natural polymers for 3D printing varies depending on which physical and chemical characteristics are to be exploited such as chemical crosslinkability, temperature sensitivity, or others. In addition to the inherent characteristics of natural polymers, the selection of bioink is printing method dependent. For instance, extrusion-based printing and SLA are capable of printing hydrogels, micro-carriers, tissue spheroids, cell pellets, tissue strands, and decellularized matrix components (5, 14). Here, we classify natural polymers for 3D printing into two categories based on their basal components such as proteins and polysaccharides. Natural polymers include collagen, gelatin, elastin, fibrinogen, and Matrigel are protein derived, while cellulose, alginate, hyaluronic acid, agarose, and chitosan are polysaccharide derived polymers. Collagen is one of the generally used proteins in tissue engineering as it is the

most abundant protein of ECM in the human body (29). Among 28 different types of identified collagen, type-I collagen occupies the largest portion in the mammalian body and cell culture. Gelatin is a derivative of collagen obtained via partial hydrolysis of collagen (30). In previous studies, gelatin has demonstrated an important role *in vivo* for its biodegradability and a sacrificial template in vascularization by using its temperature sensitivity (21, 22, 31). Fibrinogen is a protein that has been extracted from the bloodstream. Once fibrinogen is combined with the enzyme thrombin, it forms monomeric fibrin (32). Due to its superb cytocompatibility, many researchers have utilized fibrinogen in the form of fibrin to promote cell adhesion in their studies (32, 33). Matrigel is a mixture of ECM proteins secreted from Englebreth-Holm-Swarm mouse sarcoma cells (34, 35), and is notable for its ability to mimic the ECM of various cancer and stem cell lines, as well as its capacity to maintain the stem cells in an undifferentiated state (35).

Similarly, polysaccharide derived polymers possess the same biomimicry of natural polymers. Alginate (alginic acid) is a polysaccharide refined from brown seaweed and composed of (1–4)-linked  $\beta$ -D-mannuronic acid and  $\alpha$ -L-guluronic acid monomers (36). Alginate is capable of forming ionic hydrogels with moderate cell attraction (5, 36). In order to enhance cell adhesion of native alginate, prior studies introduced covalent modification (37). Hyaluronic acid (HA) or hyaluronan is a key component of the ECM, and therefore has been clinically used in the past decades. HA is composed of (1–4)-linked  $\beta$ -D-glucuronic acid and (1–3)-linked  $\beta$ -N-acetyl-D-glucosamine residues (38). Unmodified HA has several limitations to be used as a bioink due to its high viscosity and weak formability so that it requires chemical modifications and mixing with a photocrosslinkable material such as methacryloyl to induce crosslinked formation (39). Agarose is another type of polysaccharide-based natural polymer, which is derived from red seaweed and is largely composed of (1–3)- $\beta$ -D-galactopyranose-(1–4)-3, 6-anhydro- $\alpha$ -L-galactopyranose units (40, 41). Due to its poor capacity to promote cell adhesion and proliferation, agarose normally undergoes chemical modification or combination with other biocompatible polymers to be used for the scaffold fabrication. One of the reported techniques to promote cellular adhesion and mechanical stability of agarose is blending agarose with gelatin (42). Chitosan is created by alkaline hydrolysis of chitin from the shells of crustaceans and consists of  $\beta$ -(1–4)-linked N-acetyl-D-glucosamine and D-glucosamine subunits (43). Chitosan offers multiple options for chemical modifications due to its unique characteristics, such as pH-sensitive solubility, hydrophilicity, and biocompatibility (41). As a result, chitosan has been successfully exploited in many tissue engineering studies (44, 45).

With regards for the aspect of natural ECM biomimicry, decellularized extra-cellular matrices (dECM) are excellent candidates for tissue-specific bioinks. There have been a number of dECM based bioink preparation protocols reported, and researchers have utilized them for both vasculature and other cell studies (46–48). To promote the printability and cell viability of dECM based bioinks, it is a common practice to blend them with synthetic polymeric hydrogels or covalent crosslinkers (46, 49, 50).

### 3.2 Synthetic Polymers

The biggest advantage of synthetic polymers over natural polymers is controllability of their physical and chemical properties, which implies they can be custom-formulated for (51) particular printing platforms and methods. However, synthetic polymers also exhibit limitations which inhibit their greater usability such as a lack of biocompatibility, toxic degradation, and loss of mechanical properties during degradation (13).

Here, we focus on the prevalent synthetic polymers for 3D printing inks that have been used. Among the variety of bioinks available, polylactic acid (PLA) exhibits biodegradability, nontoxicity, printability, easy processability, and biocompatibility so that it has become the outstanding synthetic polymer for use in FDM printing (51–53). However, high processing temperature limits its availability for cell-laden bioprinting. Additionally, PLA has insufficient mechanical strength and bioactivity for utilization in bone replacement, so it is necessary to be used in combination with other biocompatible ceramics (52).

Polycaprolactone (PCL) has also attracted many researchers as it offers nontoxicity and low liquefaction temperature, which lead to easy blending with other natural polymers and relatively higher cell viability for extrusion-based printing (54). Polyethylene glycol diacrylate (PEGDA) is also used for cell-laden bioprinting, due to its excellent crosslinkability under UV or visible light exposure although it is not degradable material. PEGDA is commonly combined with photo-crosslinkable natural polymers such as gelatin methacryloyl (GelMA) to improve biodegradability and bioactivity (55). Polypropylene fumarate (PPF) is a biocompatible and biodegradable polymer and possesses photocrosslinkability, so it is suitable for SLA based 3D fabrication techniques. In a recent study, PPF was used as a favored material for vascular study which includes venous and aortic graft models (56). As mentioned in the previous section, Pluronic® F127 is one of the promising candidates among synthetic polymers for sacrificial templates for 3D vascular fabrication study. Pluronic® F127 belongs to the poloxamer class of polymers, which are nonionic triblock copolymers composed of polyoxypropylene (PPO) bridging two polyoxyethylenes (PEO) to maintain PEO/PPO ratio of 2:1 by weight (57). As a fugitive ink, the concentration of aqueous Pluronic® F127 solution must be greater than 20%, which is the transitional point to exhibit temperature sensitive gelation behavior (57). Chemically modifying Pluronic® F127 through acrylation or methacrylation offers greater crosslinkability under UV or visible light exposure, which enhances its benefit as a bioink (5). The combination of the two properties, thermal reversibility of gelation and photocrosslinkability, allows Pluronic® F127 to be employed for patterning of 3D vascular networks (23).

### 3.3 Cell Sources

The choice of cell types is extremely significant to construct the intended tissue with its associated functionality. As such different tissues and organs consist of various types of cells with multiple biological functions that must be recapitulated in the regenerated tissue (5, 13). Besides, the primary functional cells, most tissues contain multiple ancillary functional cell types to provide supportive, structural or barrier functions for vascularization or provide a necessary environment for stem cell maintenance and differentiation (13). To that end, it is essential to take into account that the choice of cells for 3D printing incorporates the

functionalities of primary and other cells as well as the interactions between them. Cells chosen for 3D printing are expected to mimic their behavior and functionalities *in vivo* such as cellular homeostasis, self-renewability, responsiveness to tissue damage, and integration with host tissue (5, 13, 58). The proper control of cell proliferation *in vivo* and *in vitro* is also significant since an insufficient number of cells may result in the loss of tissue and cell viability, whereas the excessive proliferation may result in hyperplasia or apoptosis (13).

The preferable source of cells is autologous due to their adaptability and minimal immune response, as they are obtained via reprogramming or differentiation of autologous stem cells. However, there are constraints for autologous and many primary cells to be utilized in 3D printed constructs, which involves the isolation of cells to be used in the *in vitro* environment and their finite lifespan (5, 13). Stem cells, such as human embryonic stem cells (ESCs) and human induced pluripotent stem cells (iPSCs), are key cell sources to overcome the obstacles associated with the current cell reservoirs. ESCs and iPSCs exhibit the capability to differentiate into unlimited lineages, which include ECs, cardiomyocytes, chondrocytes, osteoblasts, hepatocytes, insulin-secreting beta cells, and neural cells (59). Specifically, in the case of vascularization studies, it is critical to understand that native blood vessels vary in dimension and number of layers. Therefore, it is apparent that the cell composition of each layer may differ. Among all types of cells, ECs are the basic components of the innermost layer of native blood vessels (5). The presence of ECs is ubiquitous in the entire vascular network from arteries to capillaries. Also, they play a critical role in angiogenesis, vasoconstriction, and vasodilation. Therefore, ECs are of the most important cell-type to consider for vascularization study (1). EPCs from bone-marrow, are known as supportive cell sources for angiogenesis and differentiation toward ECs (1, 60). Along with ECs, the main cell components of the middle layer of large vessels, smooth muscle cells (SMCs), can also be utilized for angiogenesis due to their self-assembly capability (5). In addition, co-culture systems using multiple types of cells to improve vascular network generation have been widely used in related studies. For instance, human mesenchymal cells (hMSCs) can be co-cultured with ECs to promote angiogenesis and cell viability in cardiovascular studies (1, 61).

In 3D printing of tissues or organs, cells can be directly encapsulated in bioinks during the printing process or seeded on 3D constructs after printing. For direct cell encapsulation, they must present robustness to endure physical and biological stresses including the existence of external forces, pressure, and others (13). In post seeding, the positioning of cells at the desired location of the fabricated 3D construct remains a critical challenge (5).

#### 4. Vascular Network Fabrication and Applications

To preserve and mimic the metabolic functions of native tissues, including transportation of nutrients and oxygen, as well as the removal of cellular waste and CO<sub>2</sub>, the robust formation of a perfusable vascular network is significant for 3D printed tissues or organs (9). For example, cells located further than 200  $\mu\text{m}$  from the closest capillaries experience hypoxia and apoptosis due to limited oxygen and nutrient supply (5, 8). It is known that native blood vessels vary in scale from centimeters (aorta) to microns (capillaries) with different blood pressures (18). As mentioned above, the native blood vessels are classified into three major



components: 1) arteries (arterioles), 2) capillaries, and 3) veins (venules). Arteries hold the highest blood pressures and transport blood from the heart, while veins carry blood back to the heart, and capillaries bridge them. The blood vessels consist of three primary layers, tunica adventitia, tunica media, and tunica intima. The outmost layer, tunica adventitia, is comprised of collagen, fibroblasts, and ECM. The tunica media, the middle layer is the thickest layer and primarily consists of SMCs and pericytes, which demonstrate distinctive cardio-protective functions such as angiogenic generation and chronic inflammation reduction. The tunica intima is the innermost vascular layer and is comprised of ECs. It is responsible for conducting blood flow regulation, as well as platelet and leukocyte control (62).

Hierarchical integration of the listed features above within a 3D printed structure is currently incomplete as it requires precise geometric and functional controls over fabrication, especially at the submicron scale. Herein, we mainly introduce the current techniques for modeling a 3D vascular network incorporated into tissues and organs, such as vascularized bone, vascularized skeletal muscle, cardiovascular system, liver, and brain to analyze their innovativeness in biofabrication of complicated structural and functional characteristics.

#### 4.1 Vascularized Bone

In the human body, bone tissue is highly vascularized and metabolically active, and is comprised of a rigid natural composite of collagen and hydroxyapatite. It is classified into two mineralized tissues, cortical bone which has 10–30% porosity and a hard outer layer, and cancellous bone with a 30–90% porosity interior (63). Such a vascularized system enables the supply of nutrients, oxygen, and blood, as well as the removal of waste products to preserve skeletal coherence (64, 65). For this reason, intraosseous vasculatures in the human body stay within 100  $\mu\text{m}$  from their closest capillaries. Otherwise, insufficient blood supply by incomplete vascularization will result in avascular necrosis. In addition, intraosseous vasculature offers advanced functions to maintain skeletal integrity, such as bone remodeling, development, and fracture repair (66).

Traditionally, an ideal bone graft model was expected to possess a number of properties including osteointegration, osteoconduction, osteoinduction, and osteogenesis (67). Since the 3D printing technique has attracted many researchers as a superb substitute for traditional bone graft fabrication, various studies have demonstrated the importance of vascularization for 3D bone printing. As a result, vasculogenesis and angiogenesis have become characteristic processes that must be taken into account for the design of 3D bone regeneration studies. Wang *et al.* demonstrated a method using a virus-activated matrix (VAM) with arginine-glycine-aspartic acid (RGD) peptide phage nanofibers incorporated 3D printing to induce vascularized osteogenesis. In their study, the rat mesenchymal stem cell (rMSC) seeded scaffold was used as a bone void filler and generated new blood vessels in the bone defect area (64). The researchers in our lab, Holmes *et al.*, previously performed nanocrystalline hydroxyapatite (nHA) incorporated microfeatured vascularized bone scaffold (68). Temple *et al.* designed and fabricated anatomically shaped vascularized bone grafts with PCL, which is synthetic and biodegradable, and human adipose-derived stem cells (hASCs) using 3D printing technology (69). Similarly, Yan *et al.* recently reported a

study of PCL-based, vascularized 3D printed bone scaffolds that can control the release of deferoxamine (DFO), which is regarded as a desirable material to enhance vascularization and bone regeneration (70–72). A PLGA and nHA based 3D biplotting technique to fabricate hyperelastic vascularized bone has also been recently reported (73). In our lab, we have successfully created an engineered vascularized bone with a fluid perfusable microstructure by 3D FDM printing. A biologically inspired nanocoating technique was incorporated into the 3D printed scaffolds, in order to obtain the smart delivery of dual growth factors (BMP-2 and VEGF) with the sequential release in spatiotemporal coordination (Figure 2a–d) (2). In another recent study, we proposed an integrated approach for complex vascularized bone regeneration, which combines an advanced dual 3D printing platform with regional immobilization strategies of bioactive factors. The combination of hard PLA bone scaffolds and soft GelMA vessels provided a promising platform to obtain a hierarchically biomimetic construct, with multiphasic characteristics (Figure 2e–i) (3). These approaches present clinical potential to generate biomimetic vascularized bone grafts with complex 3D structure and biocompatible functionalities.

## 4.2 Vascularized Skeletal Muscle

Muscles are primarily responsible for the movement control and force generation through tendons by contraction as they are bonded to bones or internal organs (74). Muscles including skeletal muscles, cardiac muscle (myocardium), and smooth muscles are mainly comprised of muscle fibers, which consists of myofibrils with myofilaments as sub-composites and interweaved high-density vessels (74). Among the three major muscle types, skeletal muscles are attached to bones directly or indirectly via tendons, which have been independently investigated for the development of artificial fabrication techniques, while cardiac and smooth muscles are commonly combined with the corresponding internal organs. Vascular networks are directly linked to the primary role of skeletal muscles, the actuation of contraction.

In order for 3D printed skeletal muscles to possess therapeutic potential, seamless propagation of applied load must be taken into account, as natural skeletal muscles are capable of achieving efficient force transmission (74). In addition, natural muscle, like bone, is a highly vascularized tissue type and accounts for most of the energy consumption in the human body. In other words, more precise control and even dispersion of the vascular network fabrication are required for 3D printed skeletal muscles to perform adequate force delivery.

Many researchers have utilized genetically modified myoblasts or growth factor delivery matrices to enhance vascularization on fabricated skeletal muscle tissue (75–78). For example, Von Degenfeld *et al.* demonstrated an approach to generate new blood vessels using myoblasts with growth factors including VEGF and fibroblast growth factor (FGF) (77). After the transition to the 3D printing era, a number of techniques have been utilized to generate vascularized muscle tissue constructs. Levenberg *et al.* engineered vascularized skeletal muscle tissues *in vitro* by co-culturing myoblasts, embryonic fibroblasts, and ECs in poly-(L-lactic acid) (PLLA) and PLGA based 3D scaffolds (75). Their results have shown

that pre-vascularized skeletal muscle tissues generated by an endothelial co-culture system help induce vascular networks *in vivo* (Figure 3).

### 4.3 Vascularized Skin

The skin accounts for approximately 16% of the body's weight and is the primary component of the integumentary system of the human body (79). The most common misunderstanding with regard to the skin and its accessory structures is that they belong are a single type of tissue. In fact, the skin consists of multiple layers of tissues and is classified as the largest organ of the human body, and provides the outmost barrier against the environment and pathogens (47, 79). The human skin consists of three primary layers: the epidermis, dermis, and hypodermis, with each having various subdivisions (79).

Fabrication of artificial skin has been actively pursued for cosmetic and therapeutic purposes, such as substitution of skin loss or defects. Before significant attention had been drawn towards the 3D printing approach, and even still in the present day, autografts and allografts have been the most prevalent treatment for large skin injuries (80). However, limited donor site supply for autografts and potential risk of unexpected transplant rejection for allografts have accelerated the need for an alternative solution (80). As a result, a number of studies for vascularized skin with 3D printing have been performed. (47, 81–83)

In the recently reported study by Kim *et al.*, porcine skin-derived dECM was utilized as a raw material in a bioink to fabricate a 3D printed pre-vascularized skin patch. In their study, extrusion-based and inkjet-based 3D printing techniques were exploited to model the human dermis and epidermis in a layer-by-layer fashion for an *in vitro* experiment. Simultaneously, hASCs and EPCs laden bioinks were used in the creation of the pre-vascularized skin patch for *in vivo* study (47). Michael *et al.* used a laser-assisted 3D printing technique to engineer skin substitutes *in vivo*. The multiple layers of fibroblast-based and keratinocyte-based collagen were 3D printed onto a sheet of the stabilization matrix. In their study, vascularization was promoted by the presence of keratinocytes, which are known to generate VEGF (81, 84). Moreover, Skardal *et al.* utilized a direct 3D printing approach of amniotic fluid-derived stem cells to promote vascularization of skin *in vivo* (82). These 3D printing-based experimental results have suggested the use of different cellular approaches to conventional cell-based methods, which typically include ECs or MSCs for the fabrication of vascularized skin.

### 4.4 Cardiovascular System

The cardiovascular system includes the heart, blood vessels (arteries, veins, arteriovenous shunts, and capillaries), and lymphatic vessels (1). Based on the statistics provided by the American Heart Association (AHA), cardiovascular disease (CVD) directly or indirectly accounts for beyond 55% of all deaths in the United States, and has been the No. 1 reason for death since 1900 (85). Although CVD has been recognized as the primary risk of decreasing the average life expectancy during the past century, the clinical approaches incorporating organ transplantation still experience remaining challenges due to a lack of donor tissue.

The primary organ of the cardiovascular system, the heart consists of several types of cardiac tissues such as myocardium, endocardium, and pericardium (86). The myocardium is a thick muscle wall, composed of cardiomyocytes (or cardiac muscle cells) to perform contraction and relaxation to supply blood (5). The endocardium lies in the innermost layer and primarily consists of ECs, and the pericardium is a double-walled layer which covers the exterior of the heart (86). A high-density capillary network ( $3000/\text{mm}^2$ ) is located in the myocardium a functions to regulate the metabolic activity of contraction, and works to confine the distance between cardiomyocytes and ECs within a range of 2–3  $\mu\text{m}$ . Additionally, the blood vessels in the cardiovascular system have complex tree-shape structures, and exhibit vessel diameters in the range of ~5–10  $\mu\text{m}$  for the smallest capillaries, to 30 mm for the largest artery (1). Therefore, along with the development of 3D vascularized network, the replacement of these cardiovascular tissues using 3D printing technology has been considered as an important issue in the clinical perspective.

**4.4.1 Perfusable Vascular Networks**—As mentioned above, the absence of perfusable vascular networks in 3D printed scaffolds ultimately leads to necrosis of core tissue, referred to as avascular necrosis, which results from over population of seeded cells and a lack of nutrition and oxygen supply (87). One of the reported studies to fabricate 3D printed perfusable vascular tubes used a coaxial extrusion platform with a blended bioink of GelMA, sodium alginate, and 4-arm poly(ethylene glycol)-tetra-acrylate (PEGTA) (88). In this study, 3D printed perfusable blood vessels were created in various diameters and shapes to prove physical and biological stabilities. Miller *et al.* have created 3D multiscale interconnected vascular networks with carbohydrate glass as a sacrificial material using extrusion-based 3D printing. They demonstrated the key components of vascularized tissues including a vascular lumen, human umbilical vein endothelial cells (HUVECs), and cells matrix in the interstitial zone (87). Cui *et al.* used a modified 3D thermal inkjet printer to fabricate microvasculature. The authors utilized the simultaneous deposition of human microvascular endothelial cells (HMVECs), which are capable of forming capillaries, and fibrin, which has the capability of wound healing and promoting cell migration (89). This study demonstrated the integrated formation of perfusable microvasculature as cells proliferate. Thus, their approach can be considered for cardiovascular networks formation based on 3D thermal inkjet printing.

**4.4.2 Vascularized Cardiac Tissues**—Along with a notable focus on the fabrication of perfusable tubular constructs, there have been a number of investigations on integrated cardiac tissues. For example, Zhang *et al.* performed 3D double crosslinked printing of vascularized myocardial constructs (90). In order to generate blood vessels, they utilized the combination of the two aforementioned approaches including vasculogenesis and angiogenesis using the self-promotion of ECs and direct fabrication using the 3D printing technique (90). Their strategy to encapsulate ECs in the 3D printed microfiber structure offers a convincing approach to develop hydrogel based vascular myocardial tissues. Moreover, our lab recently developed novel gelatin-based 3D printed vascular constructs with two distinctive layers that are comprised of ECs and SMCs. As shown in Figure 4, the uniform distribution of ECs and SMCs was demonstrated inside and outside the lumen, respectively. In addition to that, the 3D printed vascular constructs have shown outstanding

abilities of myogenesis and vasculogenesis. In another recent study, we fabricated a 3D printed vascularized cardiac patch and successfully implanted into the infarcted heart of mice (Figure 4). The experimental results prove that our innovative techniques possess the feasibility to create biomimetic structures for cardiac tissue regeneration.

Most of the current 3D printed cardiovascular systems primarily lack mechanical robustness due to the inherent mechanical characteristics of their bioink materials, especially when hydrogels are used (91, 92). The poor mechanical properties of the hydrogels in comparison to the native blood vessels and valves of the cardiovascular system are considered to be the biggest impediment to successful 3D cardiac printing. The limited mechanical strength of hydrogels leads to poor structural integrity and clinical failure after implantation. As such, prospective research with emphasis on the development of new suitable materials is ultimately required. In the same context of structural integrity, another considerable challenge to fabricate translational 3D printed vascularized cardiac tissues is the electrophysiological connection of cardiomyocytes to determine the proper activity of the sinoatrial node as a pacemaker (93). From the 3D printing techniques perspective, 3D inkjet-based printed cardiovascular systems are restricted to low viscosity bioinks to prevent nozzle clogging. On the contrary, bioinks with high viscosity are only applicable for extrusion-based 3D printing of cardiovascular systems, which results in poor cell viability. Cell-laden cardiovascular systems that are 3D printed by the SLA method often result in poor cell viability due to both the DNA damage incurred by resident cells during the UV photocrosslinking process, and the cytotoxicity caused by various photoinitiators (1).

#### 4.5 Liver

The liver is considered one of the most significant organs in the human body due to its special characteristics. The liver is responsible for a number of important roles related to metabolism and metabolic regulation, such as filtration of blood from the digestive tract, detoxification of chemicals, accessory digestion, and nutrient storage in the form of glycogen (5, 79). The liver is primarily classified into two major lobes, left and right lobes. The right lobe, which is much bigger than the left lobe, involves two minor lobes such as quadrate and caudate lobes. Blood is supplied to the liver through two different vessels. The hepatic artery supplies arterial blood from the heart to the liver, and the hepatic portal vein carries blood consisting of nutrients and toxins from the intestines to the liver (79).

Previously, Griffith *et al.* fabricated a vascularized liver on a small scale with the 3D printing technique (6). Up until now, many tissue engineers have attempted to fabricate biomimetic 3D printed vascularized liver constructs with the incorporation of the characteristics listed above and its own unique properties such as a rapid restoration ability even after considerable damage (94). For example, 3D printing of hepatocytes using a hydrogel has been introduced (95). Robbins *et al.* from one of the 3D printing companies for human tissue, Organovo™, presented *in vitro* models of 3D vascularized liver. The researchers demonstrated a multi-cellular liver structure involving hepatocytes, hepatic stellates, and ECs (96). The liver transplantation into the patient's body performed by Zein *et al.* also proved the validity of the 3D printing techniques for the vascularized liver. Prior to the transplantation, the dimensions of the donor and recipient livers in detail were recorded

including the diameters of veins to fabricate a vascularized liver using the 3D printing technique. To implement the external vascularization, the authors utilized a permanent adhesive to attach to the liver lobe (Figure 5) (7). These results demonstrate the potential efficacy of a 3D printed synthetic liver with a vascular network in the human body as a valuable tool for drug delivery and a substitute for treating partially or irreversibly damaged liver tissue.

#### 4.6 Brain

The brain, along with the spinal cords, is the main component of the human central nervous system (CNS). Although the peripheral nervous system (PNS), which accounts for the rest of the nervous system, possesses the capacity of innate regeneration, the CNS remains permanently damaged after severe injury due to the glial scar formation (gliosis) (97). The brain consumes approximately 25 percent of the total amount of oxygen in the human body to maintain its functionality as the command center. Therefore, sufficient blood supply is a critical requirement, as the brain is comprised of a complex vascularized system (79, 98). Furthermore, the brain has a distinctive mechanism called the blood-brain barrier (BBB), which is formed by brain ECs, to regulate the microenvironment (99). Considering these special characteristics and importance, the 3D printing technique for a replicable brain has attracted many researchers.

The blood is supplied into the brain via two major pairs of arteries, which are vertebral and internal carotid arteries. A pair of vertebral arteries merge into the basilar artery, and divided further into the posterior cerebral and superior cerebellar arteries. The internal carotid arteries also split into the middle and anterior cerebral arteries. Ultimately, the internal carotid and basilar arteries converge into the circle of Willis (cerebral arterial circle) (79, 98). In 3D printing of neural tissues, one of the most crucial requirements for bioink selection is the balance of biofunctionality with biocompatibility (100–103). As neural cells possess comparably high sensibility, bioinks must exhibit cell recognition sequences to avoid potential immunological rejection after implantation (103). In addition, biomaterials with electrochemically conductive properties, such as polypyrrole (PPY) and poly-3,4-ethyenedioxythiophene (PEDOT), are worthwhile to consider since interactions between nerve cells are primarily electrochemical in nature (103–105). Carbon-based biomaterials including carbon nanotubes (CNTs) and graphene are other viable candidates for 3D printing neural tissues due to their superior capacity for neuronal cell-specific adhesion and outstanding electromechanical characteristics (100, 103).

Due to the inherent complexity of the BBB structure, the 3D printing incorporated vascularization of the brain still remains challenging. As a result, the current progress of the associated studies is mostly limited at demonstrating an external shape of the brain including skulls or focusing on the fabrication of neural networking. For instance, Naftulin *et al.* performed a study in that manner to demonstrate an FDM based 3D printed brain with synthetic polymers such as PLA and acrylonitrile butadiene styrene (ABS) (106). Lozano *et al.* designed and demonstrated a 3D printed brain shape construct using a novel peptide modified polymer, gellan gum-RGD with primary cortical neurons. Utilizing a simplified hand-held extrusion-based 3D printing system, they obtained successful results of neural

projections, networks formation, and encapsulation of cortical tissues (107). In a recent study, Xu *et al.* created a 3D printed segmental model of intracranial arteries from magnetic resonance angiography (MRA) images as a feasible solution to the intracranial stenosis (108). As noted above, studies performed in 3D printing of the vascular brain are somewhat limited by now. However, these approaches suggest the potential of 3D printing as a solid platform with further optimization and investigation to construct a functional brain replacement containing vascularized channels (Figure 6).

## 5. Conclusion and Future Direction

3D printing as integration of innovative techniques offers remarkable benefits in terms of a vascular network formation in tissue and organ. During the past years, researchers involved in tissue engineering, material science, and medicine have developed a variety of distinctive 3D printing techniques and biocompatible materials with high-throughput, long-term sustainability, and non-cytotoxicity to make the 3D printed platform functional. 3D printing has especially attracted many researchers as a non-substitutable technique for the permanent vascular network formation due to its feasibility, a variety of available printing methods, and precise controllability.

The current and prospective research in 3D printed vascularization aims to overcome several technical limitations, such as accounting for the dimensions of blood vessels. For example, capillaries in the human body vary as low as 5–8  $\mu\text{m}$  in diameter. The thickness of the blood vessel walls varies immensely as well. Therefore, improvements in printing resolution and precise controllability are necessary to generate refined features. The suitable biomaterial selection also enhances resolution, printability, biocompatibility, and cell viability as an inequivalent match of biomaterial and cell may result in poor biological functionality. In the particular case of 3D printing with multiple cell types, the choice of print material is very important (9). In addition, rapid printing speed must be taken into consideration for use in clinical applications. Despite miniaturization and simplification of native tissues and organs, the creation of 3D vasculature still takes a considerable amount of time.

Currently, many researchers contribute to the improvement of 3D printed vascular networks on a best effort basis to make the technique more commercially useful in the medical industry. As previously noted, complete 3D printing of some tissues or organs such as the liver and brain are still multiple steps away from clinical application as of now. In other words, promotion of sufficient angiogenesis for tissues and organs in a shorter time, as well as enhancement of mechanical properties of 3D printing materials for vascular networks, are the main obstacles. To overcome the addressed limitations, prospective research on the development of new methods, materials, and cells with combinations of existing components will be actively pursued. Examples of such research developments include: the introduction of a novel dual 3D printing method, a newly formed biocompatible hydrogel for structural integrity of vascular networks, and supportive novel cell sources to help ECs generate angiogenesis more reliably. Surmounting the current constraints listed above in the near future, the 3D printed vascular network will be considered a future-oriented promising technology based on its unlimited repeatability after optimization and punctuality in fabrication.

## Acknowledgments

The authors would like to thank the NIH Director's New Innovator Award 1DP2EB020549-01 for financial support.

We confirm that all authors have read the journal's authorship agreement, and that the manuscript has been reviewed by and approved by all named authors. Furthermore, confirm that all authors have read the journal's policy on disclosure of potential conflicts of interest and declare that they have no conflicts of interest.

## References

1. Cui H, Miao S, Esworthy T, Zhou X, Lee SJ, Liu C, et al. 3D bioprinting for cardiovascular regeneration and pharmacology. *Advanced drug delivery reviews*. 2018.
2. Cui H, Zhu W, Holmes B, Zhang LG. Biologically Inspired Smart Release System Based on 3D Bioprinted Perfused Scaffold for Vascularized Tissue Regeneration. *Advanced science*. 2016;3(8):1600058. [PubMed: 27818910]
3. Cui H, Zhu W, Nowicki M, Zhou X, Khademhosseini A, Zhang LG. Hierarchical Fabrication of Engineered Vascularized Bone Biphasic Constructs via Dual 3D Bioprinting: Integrating Regional Bioactive Factors into Architectural Design. *Advanced healthcare materials*. 2016;5(17):2174–81. [PubMed: 27383032]
4. Zhou X, Castro NJ, Zhu W, Cui H, Aliabouzar M, Sarkar K, et al. Improved Human Bone Marrow Mesenchymal Stem Cell Osteogenesis in 3D Bioprinted Tissue Scaffolds with Low Intensity Pulsed Ultrasound Stimulation. *Scientific reports*. 2016;6:32876. [PubMed: 27597635]
5. Cui H, Nowicki M, Fisher JP, Zhang LG. 3D Bioprinting for Organ Regeneration. *Advanced healthcare materials*. 2017;6(1).
6. Griffith LG, Wu B, Cima MJ, Powers MJ, Chaignaud B, Vacanti JP. In Vitro Organogenesis of Liver Tissue. *Annals of the New York Academy of Sciences*. 1997;831(1):382–97. [PubMed: 9616729]
7. Zein NN, Hanouneh IA, Bishop PD, Samaan M, Eghtesad B, Quintini C, et al. Three-dimensional print of a liver for preoperative planning in living donor liver transplantation. *Liver transplantation : official publication of the American Association for the Study of Liver Diseases and the International Liver Transplantation Society*. 2013;19(12):1304–10.
8. Novosel EC, Kleinhans C, Kluger PJ. Vascularization is the key challenge in tissue engineering. *Advanced drug delivery reviews*. 2011;63(4–5):300–11. [PubMed: 21396416]
9. Paulsen S, Miller J. Tissue vascularization through 3D printing: will technology bring us flow? *Developmental Dynamics*. 2015;244(5):629–40. [PubMed: 25613150]
10. Jose RR, Rodriguez MJ, Dixon TA, Omenetto F, Kaplan DL. Evolution of Bioinks and Additive Manufacturing Technologies for 3D Bioprinting. *ACS Biomaterials Science & Engineering*. 2016;2(10):1662–78.
11. Hull CW. Apparatus for production of three-dimensional objects by stereolithography. *Google Patents*; 1986.
12. Patra S, Young V. A Review of 3D Printing Techniques and the Future in Biofabrication of Bioprinted Tissue. *Cell biochemistry and biophysics*. 2016;74(2):93–8. [PubMed: 27193609]
13. Murphy SV, Atala A. 3D bioprinting of tissues and organs. *Nature biotechnology*. 2014;32(8):773–85.
14. Ozbolat IT, Hospodiuk M. Current advances and future perspectives in extrusion-based bioprinting. *Biomaterials*. 2016;76:321–43. [PubMed: 26561931]
15. Suri S, Han LH, Zhang W, Singh A, Chen S, Schmidt CE. Solid freeform fabrication of designer scaffolds of hyaluronic acid for nerve tissue engineering. *Biomedical microdevices*. 2011;13(6):983–93. [PubMed: 21773726]
16. Lin H, Zhang D, Alexander PG, Yang G, Tan J, Cheng AW, et al. Application of visible light-based projection stereolithography for live cell-scaffold fabrication with designed architecture. *Biomaterials*. 2013;34(2):331–9. [PubMed: 23092861]
17. Laschke MW, Rucker M, Jensen G, Carvalho C, Mulhaupt R, Gellrich NC, et al. Incorporation of growth factor containing Matrigel promotes vascularization of porous PLGA scaffolds. *Journal of biomedical materials research Part A*. 2008;85(2):397–407. [PubMed: 17688245]



18. Kinstlinger IS, Miller JS. 3D-printed fluidic networks as vasculature for engineered tissue. *Lab on a chip*. 2016;16(11):2025–43. [PubMed: 27173478]
19. Hinton TJ, Jallerat Q, Palchesko RN, Park JH, Grodzicki MS, Shue H-J, et al. Three-dimensional printing of complex biological structures by freeform reversible embedding of suspended hydrogels. *Science advances*. 2015;1(9):e1500758. [PubMed: 26601312]
20. Golden AP, Tien J. Fabrication of microfluidic hydrogels using molded gelatin as a sacrificial element. *Lab on a chip*. 2007;7(6):720–5. [PubMed: 17538713]
21. Lee VK, Kim DY, Ngo H, Lee Y, Seo L, Yoo SS, et al. Creating perfused functional vascular channels using 3D bio-printing technology. *Biomaterials*. 2014;35(28):8092–102. [PubMed: 24965886]
22. Zhao L, Lee VK, Yoo SS, Dai G, Intes X. The integration of 3-D cell printing and mesoscopic fluorescence molecular tomography of vascular constructs within thick hydrogel scaffolds. *Biomaterials*. 2012;33(21):5325–32. [PubMed: 22531221]
23. Wu W, DeConinck A, Lewis JA. Omnidirectional printing of 3D microvascular networks. *Advanced materials*. 2011;23(24):H178–83. [PubMed: 21438034]
24. Zhang WJ, Liu W, Cui L, Cao Y. Tissue engineering of blood vessel. *Journal of cellular and molecular medicine*. 2007;11(5):945–57. [PubMed: 17979876]
25. Malda J, Visser J, Melchels FP, Jungst T, Hennink WE, Dhert WJ, et al. 25th anniversary article: Engineering hydrogels for biofabrication. *Advanced materials*. 2013;25(36):5011–28. [PubMed: 24038336]
26. Khalil S, Sun W. Bioprinting endothelial cells with alginate for 3D tissue constructs. *Journal of biomechanical engineering*. 2009;131(11):111002. [PubMed: 20353253]
27. Yamamoto K, Takahashi T, Asahara T, Ohura N, Sokabe T, Kamiya A, et al. Proliferation, differentiation, and tube formation by endothelial progenitor cells in response to fluid shear stress. *Journal of Applied Physiology*. 2003.
28. Place ES, Evans ND, Stevens MM. Complexity in biomaterials for tissue engineering. *Nat Mater*. 2009;8(6):457–70. [PubMed: 19458646]
29. Di Lullo GA, Sweeney SM, Korkko J, Ala-Kokko L, San Antonio JD. Mapping the ligand-binding sites and disease-associated mutations on the most abundant protein in the human, type I collagen. *The Journal of biological chemistry*. 2002;277(6):4223–31. [PubMed: 11704682]
30. Hellio D, Djabourov M. Physically and Chemically Crosslinked Gelatin Gels. *Macromolecular Symposia*. 2006;241(1):23–7.
31. Kuijpers AJ, van Wachem PB, van Luyn MJ, Brouwer LA, Engbers GH, Krijgsveld J, et al. In vitro and in vivo evaluation of gelatin-chondroitin sulphate hydrogels for controlled release of antibacterial proteins. *Biomaterials*. 2000;21(17):1763–72. [PubMed: 10905458]
32. Rowe SL, Stegemann JP. Microstructure and mechanics of collagen-fibrin matrices polymerized using anrod snake venom enzyme. *Journal of biomechanical engineering*. 2009;131(6):061012. [PubMed: 19449966]
33. Rao RR, Peterson AW, Ceccarelli J, Putnam AJ, Stegemann JP. Matrix composition regulates three-dimensional network formation by endothelial cells and mesenchymal stem cells in collagen/fibrin materials. *Angiogenesis*. 2012;15(2):253–64. [PubMed: 22382584]
34. Kleinman HK, Martin GR, editors. *Matrigel: basement membrane matrix with biological activity*. *Seminars in cancer biology*; 2005: Elsevier.
35. Hughes CS, Postovit LM, Lajoie GA. Matrigel: a complex protein mixture required for optimal growth of cell culture. *Proteomics*. 2010;10(9):1886–90. [PubMed: 20162561]
36. Rowley JA, Madlambayan G, Mooney DJ. Alginate hydrogels as synthetic extracellular matrix materials. *Biomaterials*. 1999;20(1):45–53. [PubMed: 9916770]
37. Augst AD, Kong HJ, Mooney DJ. Alginate hydrogels as biomaterials. *Macromolecular bioscience*. 2006;6(8):623–33. [PubMed: 16881042]
38. Kogan G, Soltés L, Stern R, Gemeiner P. Hyaluronic acid: a natural biopolymer with a broad range of biomedical and industrial applications. *Biotechnology letters*. 2007;29(1):17–25. [PubMed: 17091377]

39. Ouyang L, Highley CB, Rodell CB, Sun W, Burdick JA. 3D Printing of Shear-Thinning Hyaluronic Acid Hydrogels with Secondary Cross-Linking. *ACS Biomaterials Science & Engineering*. 2016;2(10):1743–51.
40. Johansson B Agarose gel electrophoresis. *Scandinavian Journal of Clinical and Laboratory Investigation*. 1972;29(sup124):7–19.
41. Oliveira JT, Reis R. Polysaccharide-based materials for cartilage tissue engineering applications. *Journal of tissue engineering and regenerative medicine*. 2011;5(6):421–36. [PubMed: 20740689]
42. Sakai S, Hashimoto I, Kawakami K. Agarose-gelatin conjugate for adherent cell-enclosing capsules. *Biotechnology letters*. 2007;29(5):731–5. [PubMed: 17333466]
43. Freier T, Koh HS, Kazazian K, Shoichet MS. Controlling cell adhesion and degradation of chitosan films by N-acetylation. *Biomaterials*. 2005;26(29):5872–8. [PubMed: 15949553]
44. da Silva RM, López-Pérez PM, Elvira C, Mano JF, Román JS, Reis RL. Poly (N-isopropylacrylamide) surface-grafted chitosan membranes as a new substrate for cell sheet engineering and manipulation. *Biotechnology and bioengineering*. 2008;101(6):1321–31. [PubMed: 18980184]
45. Malafaya P, Pedro A, Peterbauer A, Gabriel C, Redl H, Reis R. Chitosan particles agglomerated scaffolds for cartilage and osteochondral tissue engineering approaches with adipose tissue derived stem cells. *Journal of Materials Science: Materials in Medicine*. 2005;16(12):1077–85. [PubMed: 16362204]
46. Pati F, Jang J, Ha DH, Won Kim S, Rhie JW, Shim JH, et al. Printing three-dimensional tissue analogues with decellularized extracellular matrix bioink. *Nature communications*. 2014;5:3935.
47. Kim BS, Kwon YW, Kong JS, Park GT, Gao G, Han W, et al. 3D cell printing of in vitro stabilized skin model and in vivo pre-vascularized skin patch using tissue-specific extracellular matrix bioink: A step towards advanced skin tissue engineering. *Biomaterials*. 2018;168:38–53. [PubMed: 29614431]
48. Kim BS, Kim H, Gao G, Jang J, Cho DW. Decellularized extracellular matrix: a step towards the next generation source for bioink manufacturing. *Biofabrication*. 2017;9(3):034104. [PubMed: 28691696]
49. Jang J, Kim TG, Kim BS, Kim S-W, Kwon S-M, Cho D-W. Tailoring mechanical properties of decellularized extracellular matrix bioink by vitamin B2-induced photo-crosslinking. *Acta biomaterialia*. 2016;33:88–95. [PubMed: 26774760]
50. Gopinathan J, Noh I. Recent trends in bioinks for 3D printing. *Biomaterials research*. 2018;22(1): 11. [PubMed: 29636985]
51. Garlotta D A literature review of poly (lactic acid). *Journal of Polymers and the Environment*. 2001;9(2):63–84.
52. Guvendiren M, Molde J, Soares RM, Kohn J. Designing Biomaterials for 3D Printing. *ACS Biomater Sci Eng*. 2016;2(10):1679–93. [PubMed: 28025653]
53. Serra T, Mateos-Timoneda MA, Planell JA, Navarro M. 3D printed PLA-based scaffolds: a versatile tool in regenerative medicine. *Organogenesis*. 2013;9(4):239–44. [PubMed: 23959206]
54. Lee H, Cho DW. One-step fabrication of an organ-on-a-chip with spatial heterogeneity using a 3D bioprinting technology. *Lab on a chip*. 2016;16(14):2618–25. [PubMed: 27302471]
55. Ouyang L, Highley CB, Sun W, Burdick JA. A Generalizable Strategy for the 3D Bioprinting of Hydrogels from Nonviscous Photo-crosslinkable Inks. *Advanced materials*. 2017;29(8).
56. Melchiorri AJ, Hibino N, Best CA, Yi T, Lee YU, Kraynak CA, et al. 3D-Printed Biodegradable Polymeric Vascular Grafts. *Advanced healthcare materials*. 2016;5(3):319–25. [PubMed: 26627057]
57. Bohorquez M, Koch C, Trygstad T, Pandit N. A study of the temperature-dependent micellization of pluronic F127. *Journal of colloid and interface science*. 1999;216(1):34–40. [PubMed: 10395759]
58. Mandrycky C, Wang Z, Kim K, Kim D-H. 3D bioprinting for engineering complex tissues. *Biotechnology advances*. 2016;34(4):422–34. [PubMed: 26724184]
59. Higuchi A, Ling Q-D, Kumar SS, Chang Y, Alarfaj AA, Munusamy MA, et al. Physical cues of cell culture materials lead the direction of differentiation lineages of pluripotent stem cells. *Journal of Materials Chemistry B*. 2015;3(41):8032–58.

60. Badorff C, Brandes RP, Popp Rd, Rupp S, Urbich C, Aicher A, et al. Transdifferentiation of blood-derived human adult endothelial progenitor cells into functionally active cardiomyocytes. *Circulation*. 2003;107(7):1024–32. [PubMed: 12600917]
61. Singh A, Singh A, Sen D. Mesenchymal stem cells in cardiac regeneration: a detailed progress report of the last 6 years (2010–2015). *Stem Cell Research & Therapy*. 2016;7(1):82. [PubMed: 27259550]
62. Nemen-Guanzon JG, Lee S, Berg JR, Jo YH, Yeo JE, Nam BM, et al. Trends in tissue engineering for blood vessels. *Journal of biomedicine & biotechnology*. 2012;2012:956345. [PubMed: 23251085]
63. Bose S, Roy M, Bandyopadhyay A. Recent advances in bone tissue engineering scaffolds. *Trends in biotechnology*. 2012;30(10):546–54. [PubMed: 22939815]
64. Wang J, Yang M, Zhu Y, Wang L, Tomsia AP, Mao C. Phage nanofibers induce vascularized osteogenesis in 3D printed bone scaffolds. *Advanced materials*. 2014;26(29):4961–6. [PubMed: 24711251]
65. Tsigkou O, Pomerantseva I, Spencer JA, Redondo PA, Hart AR, O’Doherty E, et al. Engineered vascularized bone grafts. *Proceedings of the National Academy of Sciences*. 2010.
66. Santos MI, Reis RL. Vascularization in bone tissue engineering: physiology, current strategies, major hurdles and future challenges. *Macromolecular bioscience*. 2010;10(1):12–27. [PubMed: 19688722]
67. Moore WR, Graves SE, Bain GI. Synthetic bone graft substitutes. *ANZ journal of surgery*. 2001;71(6):354–61. [PubMed: 11409021]
68. Holmes B, Bulusu K, Plesniak M, Zhang LG. A synergistic approach to the design, fabrication and evaluation of 3D printed micro and nano featured scaffolds for vascularized bone tissue repair. *Nanotechnology*. 2016;27(6):064001. [PubMed: 26758780]
69. Temple JP, Hutton DL, Hung BP, Huri PY, Cook CA, Kondragunta R, et al. Engineering anatomically shaped vascularized bone grafts with hASCs and 3D-printed PCL scaffolds. *Journal of biomedical materials research Part A*. 2014;102(12):4317–25. [PubMed: 24510413]
70. Yan Y, Chen H, Zhang H, Guo C, Yang K, Chen K, et al. Vascularized 3D printed scaffolds for promoting bone regeneration. *Biomaterials*. 2019;190:97–110. [PubMed: 30415019]
71. Donneys A, Weiss DM, Deshpande SS, Ahsan S, Tchanque-Fossuo CN, Sarhaddi D, et al. Localized deferoxamine injection augments vascularity and improves bony union in pathologic fracture healing after radiotherapy. *Bone*. 2013;52(1):318–25. [PubMed: 23085084]
72. Potier E, Ferreira E, Dennler S, Mauviel A, Oudina K, Logeart-Avramoglou D, et al. Desferrioxamine-driven upregulation of angiogenic factor expression by human bone marrow stromal cells. *Journal of tissue engineering and regenerative medicine*. 2008;2(5):272–8. [PubMed: 18512268]
73. Liu X, Jakus AE, Kural M, Qian H, Engler A, Ghaedi M, et al. Vascularization of Natural and Synthetic Bone Scaffolds. *Cell transplantation*. 2018;27(8):1269–80. [PubMed: 30008231]
74. Merceron TK, Burt M, Seol YJ, Kang HW, Lee SJ, Yoo JJ, et al. A 3D bioprinted complex structure for engineering the muscle-tendon unit. *Biofabrication*. 2015;7(3):035003. [PubMed: 26081669]
75. Levenberg S, Rouwkema J, Macdonald M, Garfein ES, Kohane DS, Darland DC, et al. Engineering vascularized skeletal muscle tissue. *Nature biotechnology*. 2005;23(7):879–84.
76. Zisch AH, Lutolf MP, Hubbell JA. Biopolymeric delivery matrices for angiogenic growth factors. *Cardiovascular pathology*. 2003;12(6):295–310. [PubMed: 14630296]
77. Von Degenfeld G, Banfi A, Springer ML, Blau HM. Myoblast-mediated gene transfer for therapeutic angiogenesis and arteriogenesis. *British journal of pharmacology*. 2003;140(4):620–6. [PubMed: 14534145]
78. Lu Y, Shansky J, Del Tatto M, Ferland P, Wang X, Vandenberg H. Recombinant vascular endothelial growth factor secreted from tissue-engineered bioartificial muscles promotes localized angiogenesis. *Circulation*. 2001;104(5):594–9. [PubMed: 11479259]
79. Betts JG. *Anatomy and physiology*: Houston, Texas: OpenStax College, Rice University; 2013.

80. Kumbar SG, Nukavarapu SP, James R, Nair LS, Laurencin CT. Electrospun poly(lactic acid-co-glycolic acid) scaffolds for skin tissue engineering. *Biomaterials*. 2008;29(30):4100–7. [PubMed: 18639927]
81. Michael S, Sorg H, Peck C-T, Koch L, Deiwick A, Chichkov B, et al. Tissue engineered skin substitutes created by laser-assisted bioprinting form skin-like structures in the dorsal skin fold chamber in mice. *PLoS one*. 2013;8(3):e57741. [PubMed: 23469227]
82. Skardal A, Mack D, Kapetanovic E, Atala A, Jackson JD, Yoo J, et al. Bioprinted amniotic fluid-derived stem cells accelerate healing of large skin wounds. *Stem cells translational medicine*. 2012;1(11):792–802. [PubMed: 23197691]
83. Bibb R, Nottrodt N, Gillner A. Artificial vascularised scaffolds for 3D-tissue regeneration – a perspective of the ArtiVasc 3D Project. *International Journal of Bioprinting*. 2016;2(0).
84. Ballaun C, Weninger W, Uthman A, Weich H, Tschachler E. Human keratinocytes express the three major splice forms of vascular endothelial growth factor. *Journal of investigative dermatology*. 1995;104(1):7–10. [PubMed: 7798644]
85. Thom T, Haase N, Rosamond W, Howard VJ, Rumsfeld J, Manolio T, et al. Heart disease and stroke statistics--2006 update: a report from the American Heart Association Statistics Committee and Stroke Statistics Subcommittee. *Circulation*. 2006;113(6):e85–151. [PubMed: 16407573]
86. Tomanek RJ, Runyan RB. *Formation of the heart and its regulation*: Springer Science & Business Media; 2012.
87. Miller JS, Stevens KR, Yang MT, Baker BM, Nguyen D-HT, Cohen DM, et al. Rapid casting of patterned vascular networks for perfusable engineered three-dimensional tissues. *Nature materials*. 2012;11(9):768. [PubMed: 22751181]
88. Jia W, Gungor-Ozkerim PS, Zhang YS, Yue K, Zhu K, Liu W, et al. Direct 3D bioprinting of perfusable vascular constructs using a blend bioink. *Biomaterials*. 2016;106:58–68. [PubMed: 27552316]
89. Cui X, Boland T. Human microvasculature fabrication using thermal inkjet printing technology. *Biomaterials*. 2009;30(31):6221–7. [PubMed: 19695697]
90. Zhang YS, Arneri A, Bersini S, Shin SR, Zhu K, Goli-Malekabadi Z, et al. Bioprinting 3D microfibrous scaffolds for engineering endothelialized myocardium and heart-on-a-chip. *Biomaterials*. 2016;110:45–59. [PubMed: 27710832]
91. Duan B State-of-the-Art Review of 3D Bioprinting for Cardiovascular Tissue Engineering. *Annals of biomedical engineering*. 2017;45(1):195–209. [PubMed: 27066785]
92. Seol YJ, Kang HW, Lee SJ, Atala A, Yoo JJ. Bioprinting technology and its applications. *European journal of cardio-thoracic surgery : official journal of the European Association for Cardio-thoracic Surgery*. 2014;46(3):342–8. [PubMed: 25061217]
93. Borovjagin AV, Ogle BM, Berry JL, Zhang J. From microscale devices to 3D printing: advances in fabrication of 3D cardiovascular tissues. *Circulation research*. 2017;120(1):150–65. [PubMed: 28057791]
94. Taub R Liver regeneration: from myth to mechanism. *Nature reviews Molecular cell biology*. 2004;5(10):836. [PubMed: 15459664]
95. Wang X, Yan Y, Pan Y, Xiong Z, Liu H, Cheng J, et al. Generation of three-dimensional hepatocyte/gelatin structures with rapid prototyping system. *Tissue engineering*. 2006;12(1):83–90. [PubMed: 16499445]
96. Robbins JB, Gorgen V, Min P, Shepherd BR, Presnell SC. A novel in vitro three-dimensional bioprinted liver tissue system for drug development. *FASEB J*. 2013;27(872):812.
97. Gu X. Progress and perspectives of neural tissue engineering. *Frontiers of medicine*. 2015;9(4):401–11. [PubMed: 26482066]
98. Netter FH. *Atlas of Human Anatomy E-Book*: Elsevier Health Sciences; 2017.
99. Abbott NJ. Astrocyte–endothelial interactions and blood–brain barrier permeability. *Journal of anatomy*. 2002;200(6):629–38. [PubMed: 12162730]
100. Lee SJ, Zhu W, Nowicki M, Lee G, Heo DN, Kim J, et al. 3D printing nano conductive multi-walled carbon nanotube scaffolds for nerve regeneration. *Journal of neural engineering*. 2018;15(1):016018. [PubMed: 29064377]

101. Lee S-J, Esworthy T, Stake S, Miao S, Zuo YY, Harris BT, et al. Advances in 3D Bioprinting for Neural Tissue Engineering. *Advanced Biosystems*. 2018;2(4):1700213.
102. Lee SJ, Nowicki M, Harris B, Zhang LG. Fabrication of a Highly Aligned Neural Scaffold via a Table Top Stereolithography 3D Printing and Electrospinning. *Tissue engineering Part A*. 2017;23(11–12):491–502. [PubMed: 27998214]
103. Lee SJ, Esworthy T, Stake S, Miao S, Zuo YY, Harris BT, et al. Advances in 3D Bioprinting for Neural Tissue Engineering. *Advanced Biosystems*. 2018;2(4):1700213.
104. Shi Z, Gao H, Feng J, Ding B, Cao X, Kuga S, et al. In situ synthesis of robust conductive cellulose/polypyrrole composite aerogels and their potential application in nerve regeneration. *Angewandte Chemie International Edition*. 2014;53(21):5380–4. [PubMed: 24711342]
105. Heo DN, Acquah N, Kim J, Lee S-J, Castro NJ, Zhang LG. Directly Induced Neural Differentiation of Human Adipose-Derived Stem Cells Using Three-Dimensional Culture System of Conductive Microwell with Electrical Stimulation. *Tissue Engineering Part A*. 2018;24(7–8):537–45. [PubMed: 28741412]
106. Naftulin JS, Kimchi EY, Cash SS. Streamlined, Inexpensive 3D Printing of the Brain and Skull. *PLoS one*. 2015;10(8):e0136198. [PubMed: 26295459]
107. Lozano R, Stevens L, Thompson BC, Gilmore KJ, Gorkin R 3rd, Stewart EM, et al. 3D printing of layered brain-like structures using peptide modified gellan gum substrates. *Biomaterials*. 2015;67:264–73. [PubMed: 26231917]
108. Xu WH, Liu J, Li ML, Sun ZY, Chen J, Wu JH. 3D printing of intracranial artery stenosis based on the source images of magnetic resonance angiograph. *Annals of translational medicine*. 2014;2(8):74. [PubMed: 25333049]
109. Landers R, Hübner U, Schmelzeisen R, Mülhaupt R. Rapid prototyping of scaffolds derived from thermoreversible hydrogels and tailored for applications in tissue engineering. *Biomaterials*. 2002;23(23):4437–47. [PubMed: 12322962]
110. Elvin C, Danon S, Brownlee A, White J, Hickey M, Liyou N, et al. Evaluation of photo-crosslinked fibrinogen as a rapid and strong tissue adhesive. *Journal of Biomedical Materials Research Part A: An Official Journal of The Society for Biomaterials, The Japanese Society for Biomaterials, and The Australian Society for Biomaterials and the Korean Society for Biomaterials*. 2010;93(2):687–95.
111. Hellio D, Djabourov M, editors. Physically and chemically crosslinked gelatin gels. *Macromolecular Symposia*; 2006: Wiley Online Library.
112. Khunmanee S, Jeong Y, Park H. Crosslinking method of hyaluronic-based hydrogel for biomedical applications. *Journal of tissue engineering*. 2017;8:2041731417726464. [PubMed: 28912946]
113. Childers EP, Wang MO, Becker ML, Fisher JP, Dean D. 3D printing of resorbable poly(propylene fumarate) tissue engineering scaffolds. *MRS Bulletin*. 2015;40(02):119–26.
114. Chu CR, Coutts RD, Yoshioka M, Harwood FL, Monosov AZ, Amiel D. Articular cartilage repair using allogeneic perichondrocyte-seeded biodegradable porous polylactic acid (PLA): A tissue-engineering study. *Journal of biomedical materials research*. 1995;29(9):1147–54. [PubMed: 8567713]
115. Cutright DE, Hunsuck EE. Tissue reaction to the biodegradable polylactic acid suture. *Oral Surgery, Oral Medicine, Oral Pathology*. 1971;31(1):134–9.
116. Kweon H, Yoo MK, Park IK, Kim TH, Lee HC, Lee H-S, et al. A novel degradable polycaprolactone networks for tissue engineering. *Biomaterials*. 2003;24(5):801–8. [PubMed: 12485798]
117. Lee K-W, Wang S, Lu L, Jabbari E, Currier BL, Yaszemski MJ. Fabrication and characterization of poly (propylene fumarate) scaffolds with controlled pore structures using 3-dimensional printing and injection molding. *Tissue engineering*. 2006;12(10):2801–11. [PubMed: 17518649]
118. Tessmar JK, Göpferich AM. Customized PEG-derived copolymers for tissue-engineering applications. *Macromolecular bioscience*. 2007;7(1):23–39. [PubMed: 17195277]
119. Wang Z, Abdulla R, Parker B, Samanipour R, Ghosh S, Kim K. A simple and high-resolution stereolithography-based 3D bioprinting system using visible light crosslinkable bioinks. *Biofabrication*. 2015;7(4):045009. [PubMed: 26696527]

120. Weisel JW. Fibrinogen and fibrin. *Advances in protein chemistry*. 70: Elsevier; 2005 p. 247–99. [PubMed: 15837518]
121. Gao Q, Hu B, Ning Q, Ye C, Xie J, Ye J, et al. A primary study of poly (propylene fumarate)–2-hydroxyethyl methacrylate copolymer scaffolds for tarsal plate repair and reconstruction in rabbit eyelids. *Journal of Materials Chemistry B*. 2015;3(19):4052–62.
122. Lee Y, Chung HJ, Yeo S, Ahn C-H, Lee H, Messersmith PB, et al. Thermo-sensitive, injectable, and tissue adhesive sol–gel transition hyaluronic acid/pluronic composite hydrogels prepared from bio-inspired catechol-thiol reaction. *Soft Matter*. 2010;6(5):977–83.
123. Suggs LJ, Kao EY, Palombo LL, Krishnan RS, Widmer MS, Mikos AG. Preparation and characterization of poly (propylene fumarate-co-ethylene glycol) hydrogels. *Journal of Biomaterials Science, Polymer Edition*. 1998;9(7):653–66. [PubMed: 9686333]
124. Suggs LJ, Krishnan RS, Garcia CA, Peter SJ, Anderson JM, Mikos AG. In vitro and in vivo degradation of poly (propylene fumarate-co-ethylene glycol) hydrogels. *Journal of Biomedical Materials Research: An Official Journal of The Society for Biomaterials, The Japanese Society for Biomaterials, and the Australian Society for Biomaterials*. 1998;42(2):312–20.
125. Bertassoni LE, Cecconi M, Manoharan V, Nikkhah M, Hjortnaes J, Cristino AL, et al. Hydrogel bioprinted microchannel networks for vascularization of tissue engineering constructs. *Lab on a chip*. 2014;14(13):2202–11. [PubMed: 24860845]
126. Ye K, Felimban R, Traianedes K, Moulton SE, Wallace GG, Chung J, et al. Chondrogenesis of infrapatellar fat pad derived adipose stem cells in 3D printed chitosan scaffold. *PloS one*. 2014;9(6):e99410. [PubMed: 24918443]
127. Daamen WF, Veerkamp J, Van Hest J, Van Kuppevelt T. Elastin as a biomaterial for tissue engineering. *Biomaterials*. 2007;28(30):4378–98. [PubMed: 17631957]
128. Kirchmayer DM, Gorkin R Iii. An overview of the suitability of hydrogel-forming polymers for extrusion-based 3D-printing. *Journal of Materials Chemistry B*. 2015;3(20):4105–17.
129. Fan R, Piou M, Darling E, Cormier D, Sun J, Wan J. Bio-printing cell-laden Matrigel–agarose constructs. *Journal of biomaterials applications*. 2016;31(5):684–92. [PubMed: 27638155]

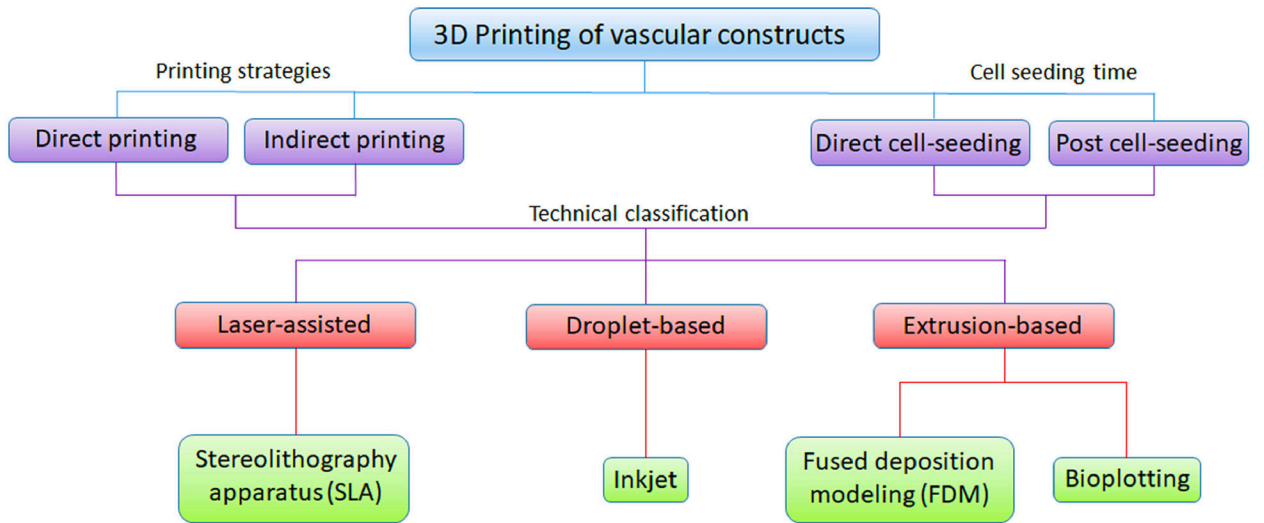


**Figure 1.** A diagram tree of the 3D printing techniques for vascular network fabrication.

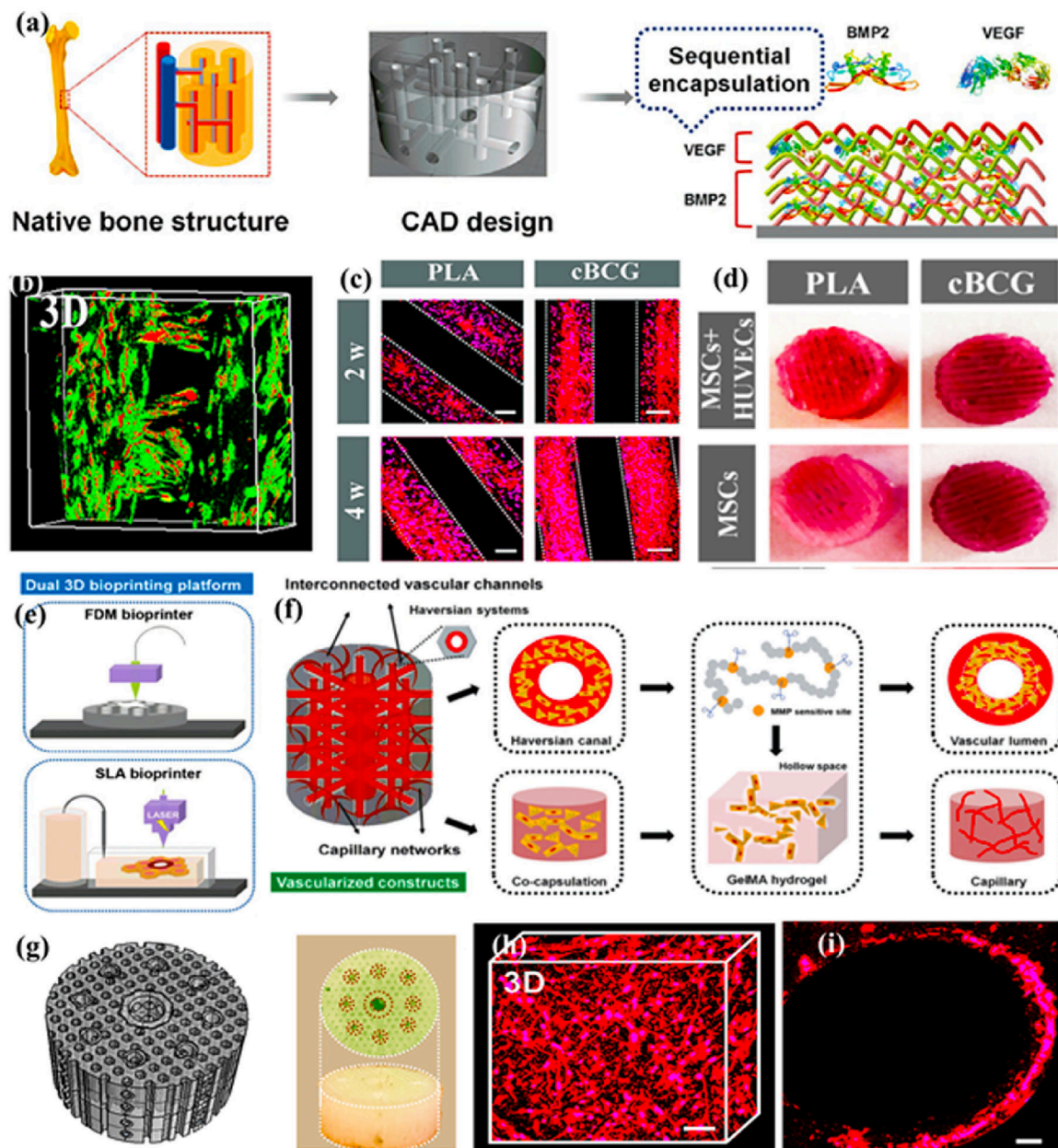


**Figure 2.**

(a) Schematic illustration of the fabrication process of 3D bioprinted vascularized bone scaffolds with bioactive growth factor nanocoatings. (b) A 3D confocal fluorescence image of hMSCs (green) and HUVECs (red) co-cultured for 5 days. (c) Immunofluorescence images of hMSCs and HUVECs with CD31 antibody for 2 and 4 weeks on different scaffolds. A PLA based control scaffolds (left) and a genipin crosslinked bioactive nanocoating with growth factors (cBCG) based scaffold (right). Scale bars, 100  $\mu$ m. (d) Mineralization of osteogenic differentiation of hMSCs and hMSCs/HUVECs on PLA and cBCG based scaffolds analyzed by Alizarin red staining. (e) Schematic illustration of a dual 3D bioprinting platform. (f) Schematic representation of the microstructural design of a biomimetic biphasic vascularized bone construct based on a matrix metalloproteinase (MMP)



sensitive GelMA hydrogel. The evolution of vascular lumen and capillary network formation can be achieved in different regions during the culture period. (g) Computer-aided design (CAD) model of the biphasic vascularized bone construct, including the bone region and vascular channels (left). Microscopic photo image of manufactured vascularized bone construct (right). Red circles show tubular vascular hydrogel regions. (h) A 3D immunofluorescence image of the vascular capillary network with CD31 antibody in the designed different regions of the 10 wt% GelMA hydrogel printed by the dual 3D bioprinting platform after 4 weeks. Scale bar, 50  $\mu\text{m}$ . (i) A 3D immunofluorescence image of a vascular lumen in the 3D bioprinted vascularized bone. Scale bar, 50  $\mu\text{m}$ . Images are adapted from (2, 3).

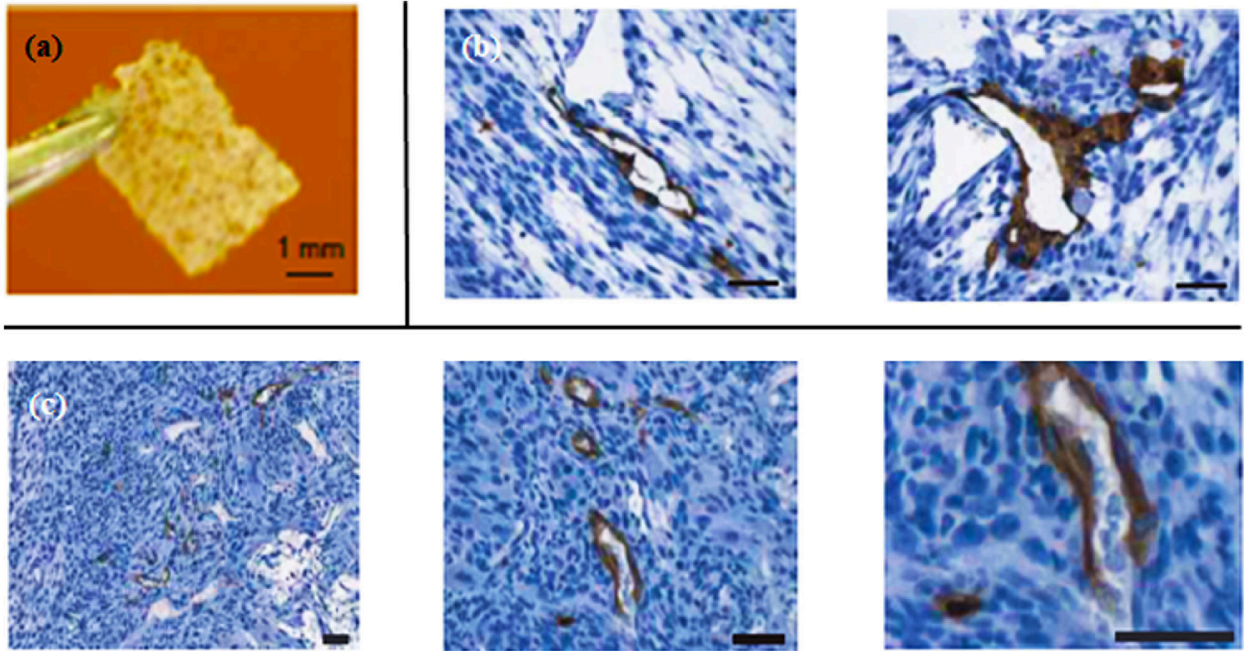


**Figure 3.**

(a) 3D printed scaffold before cell seeding. Scale bar, 1 mm. (b) Immunostaining images of vascular network generation *in vitro* within skeletal muscle construct after one month. Skeletal myoblasts, ECs, and mouse embryonic fibroblasts were tri-cultured. Scale bar, 50 μm. (c) Immunostaining images of *in vivo* study of the vascularized skeletal model after two weeks of transplantation into immunodeficient mice. The constructs underwent immunostaining with human-specific CD31 antibody. Scale bar, 50 μm. Images are adapted from (75).

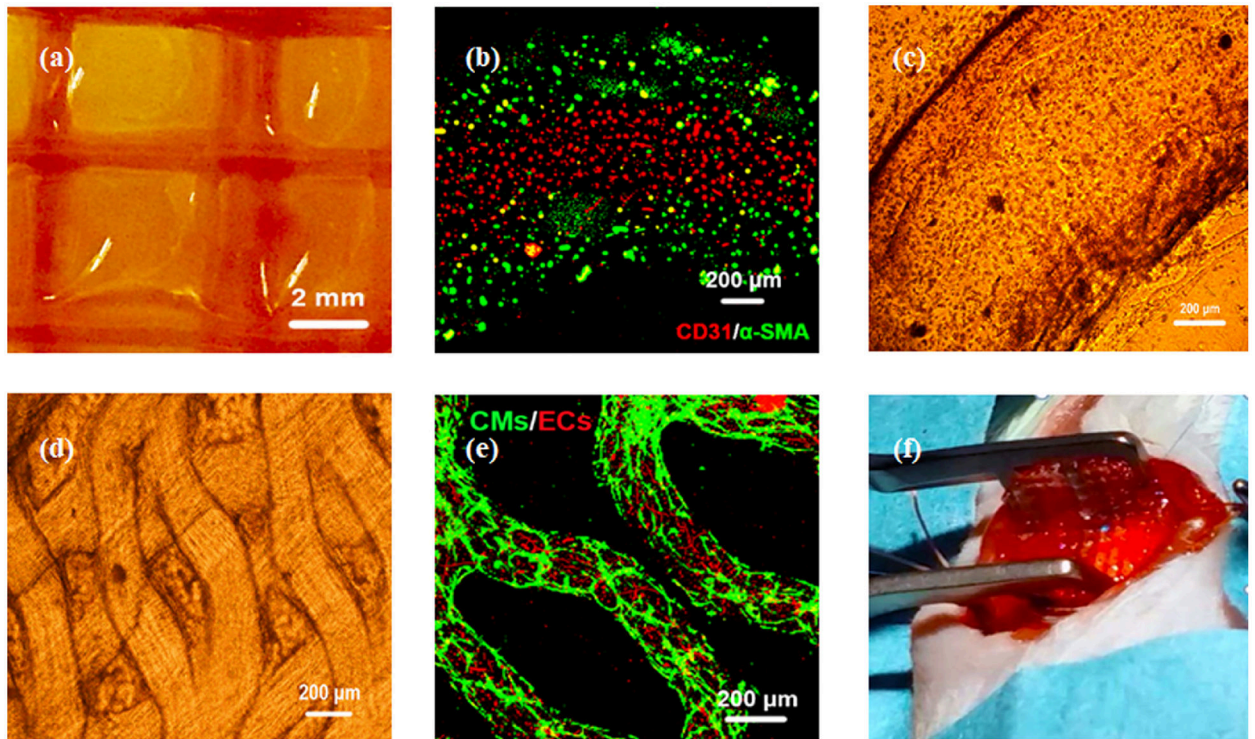


**Figure 4.**

(a) 3D printed vasculature with hollow and interconnected structure after 24 hours of perfusion culture. (b) An immunofluorescence image of 3D printed vasculature (CD 31 antibody and  $\alpha$ -smooth muscle actin ( $\alpha$ -SMA)) in a dynamic culture condition. (c) An optical microscopic image of dynamic flow in the 3D printed vasculature. (d) An optical microscopic image of anisotropic honeycomb constructs of 3D bioprinted vascularized cardiac patch. (e) A fluorescence image of 3D bioprinted vascularized cardiac patch (cardiomyocyte (CMs) and ECs). (f) *in vivo* implantation of 3D bioprinted vascularized cardiac patch into infarcted heart of mice.



**Figure 5.**

(a) Side view of 3D printed liver and extracted liver of a patient, where long, short, and double arrows indicate hepatic artery, hepatic vein, and portal vein, respectively. (b) Right lobes of 3D printed and extracted livers with indications of the hepatic artery (single arrows) and portal vein (double arrows). (c) Cross-sectional views of 3D printed and extracted livers with indications of hepatic vein (single arrows) and portal vein (dotted arrows). Images are adapted from (7).

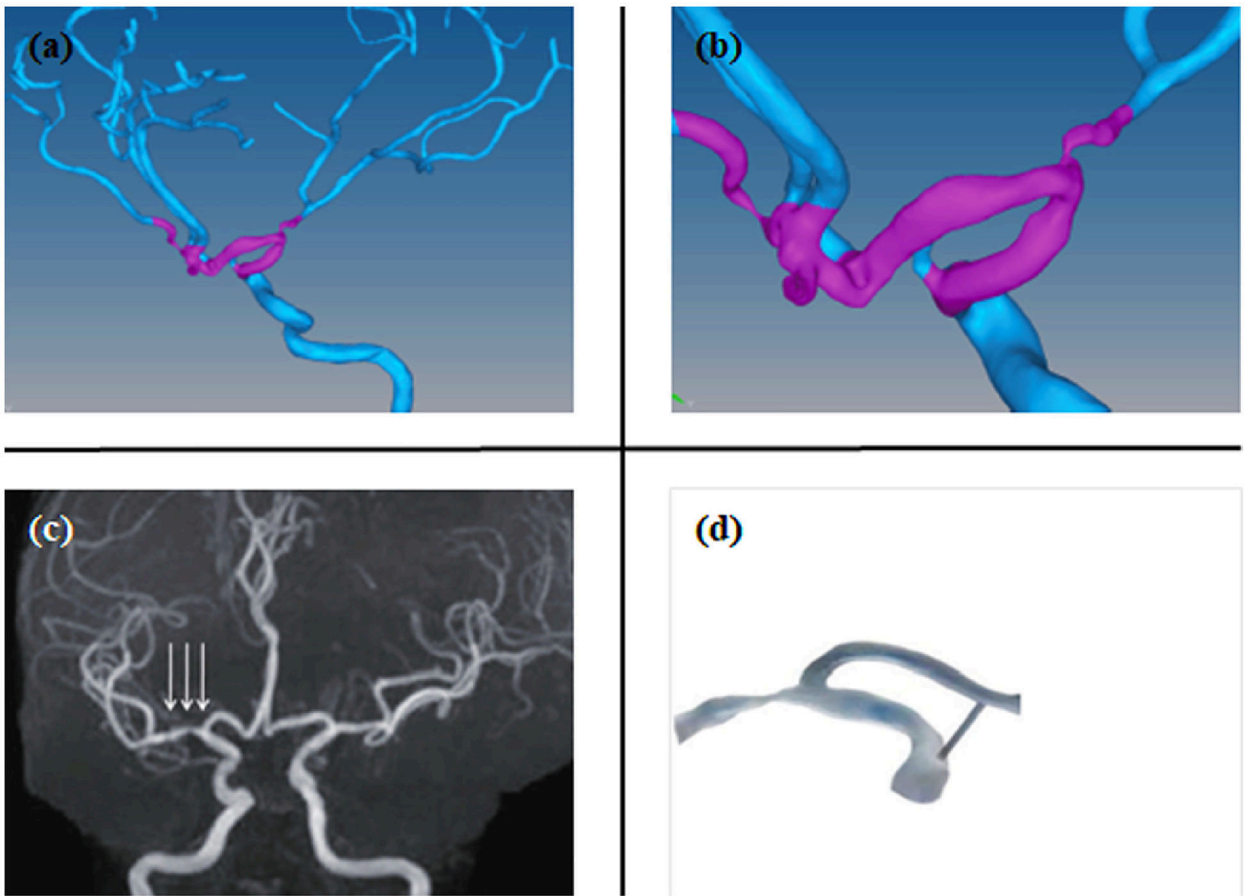


**Figure 6.**

(a) A 3D arterial construct of magnetic resonance imaging from a patient. (b) A magnified image of the highlighted region. (c) A magnetic resonance angiography image and (d) 3D printed model of the indicated region with arrows. Images are adapted from (108).

**Table 1.**

List of 3D Printing Methods for Vascular Fabrication (5, 10, 13, 14, 109)

Technical classification	Printing technique	Unique properties	Advantages	Disadvantages
Laser-assisted	Stereolithography apparatus (SLA)	Surface photopolymerization	High resolution	Limited selection for bioinks and cell damage by UV light
Droplet-based	Inkjet	Adjustable droplet size and shape	Low cost, least damage to printed cells, and rapid fabrication	Limited 3D resolution and restricted cell density
Extrusion-based	Fused deposition modeling (FDM)	Heating for state transition of materials	Good versatility and a wide selection of bioinks	Limited resolution and restricted hydrogel use
	Bioplotting	Simultaneous use of multiple bioinks	Wide selection of bioinks	Slow fabrication

Author Manuscript

Author Manuscript

Author Manuscript

Author Manuscript

**Table 2.**

List of Natural and Synthetic Materials for Bioinks (4), (5), (14), (23), (35, 38), (41, 42), (25, 46–48, 76–78, 110–129)

Material classification		Printing technique	Solidification mechanism	Strengths	Drawbacks
<b>Protein</b>	Collagen and its derivatives	Droplet, extrusion, and SLA	Physical or chemical crosslinking	Nonimmunogenic	Low cell adhesion without modification
	Gelatin and its derivatives	Droplet, extrusion, and SLA	Physical or chemical crosslinking	Nonimmunogenic	Weak mechanical properties without modification
	Elastin	Droplet and extrusion	Self-assembling	Good biocompatibility	Calcification, hydrophobicity, and insolubility
	Fibrin	Droplet, extrusion, and SLA	Self-assembling	Angiogenesis enhancement	Low mechanical property
	Matrigel	Droplet and extrusion	Self-assembling	Self-renewal and pluripotency for stem cells	Low mechanical property
<b>Polysaccharide</b>	Agarose	Droplet and extrusion	Physical crosslinking	Thermo-reversibility	Low cell adhesion without modification
	Alginate	Droplet and extrusion	Physical crosslinking	Biocompatibility, fast gelation, and nonimmunogenic	Low cell adhesion without modification
	Chitosan	Extrusion	Chemical crosslinking	pH-sensitive solubility, biocompatibility, and hydrophilicity	High viscosity
	Hyaluronic acid and its derivatives	Droplet, extrusion and SLA	Physical or chemical crosslinking	The similarity to ECM and cell viability	Poor mechanical property
<b>Decellularized ECM</b>		Droplet and extrusion	Physical or chemical crosslinking	Natural ECM biomimicry and tissue specificity	Complex preparation steps
<b>Polyethers</b>	Poly(ethylene glycol) diacrylate	SLA	Covalent crosslinking	Nonimmunogenic	Low cell adhesion
<b>Polyesters</b>	Poly(caprolactone) and its derivatives	Extrusion and SLA	Temperature or covalent crosslinking	Good biocompatibility	Very slow degradation
	Poly(lactic acid)	Extrusion	Temperature	Good biocompatibility	Immunogenicity
	Poly(propylene fumarate)	SLA	Covalent crosslinking	Good biodegradability	Immunogenicity
<b>Poloxamer</b>	Pluronic F127	Extrusion	Physical crosslinking	Nonimmunogenic and high printability	Poor mechanical property and slow gelation